CAP-1 binding site.[30] In the structure crystallized in the presence of CAP-1, the side chain of Phe32 is repositioned ~6 Å from its buried location in the protein core to a solvent exposed environment Figure 1. The Phe32 side-chain, in turn, displaces the side-chain of Tyr145 from a partly buried position within a hydrophobic hollow in the free protein to a poorly ordered conformation that is not clearly defined in electron density maps of the protein crystallized in the presence of CAP-1. In addition, electron density was not observed for the side-chain of His62, which was well defined in structures determined for the free CA^N protein.

NMR studies of CAP-1:CA^N

CAP-1 contains a urea moiety that can adopt two conformations (1 and 2; Figure 2). Positive nuclear Overhauser effects (NOEs) were observed from the CAP-1 N1-H to both the H-5 and H-6 protons of the free CAP-1 ligand (2 mM, 5% DMSO-d_6/95% H_2O), indicating that the 2-conformation is favored ([1]/[2] ~ 0.5/1) (Figure 2). NMR data were also obtained for CAP-1 in the presence of CA^N (0.100 mM; [CAP-1]/[CA^N] = 20:1). Negative transfer-NOEs were observed under these conditions, and the relative N1-H to H5 and H6 intensities shifted in favor of the 1 conformer ([1]/[2] ~ 2:1) (Figure 2). The residual N1-H to H5 signal results from rapid exchange between free (20-fold excess) and bound CAP-1 coupled with urea bond isomerization. These data indicate that the 1 conformer is preferentially, if not exclusively, bound by CA^N.

2D NOESY spectra were obtained for CA^N as a function of added CAP-1 (Figure 2(d)). Significant chemical shift changes were observed for a number of CA^N residues, including Val27, Ala31, His62, Leu138, Ile141, and Tyr145. In some cases, intramolecular NOE intensities changed significantly upon CAP-1 binding. For example, NOEs between His 62-$H^{\delta 2}$ and both Val 27-γ_1CH_3 and Val 59-γ_2CH_3 decreased upon titration with CAP-1 (Figure 2), whereas His62-$H^{\varepsilon 1}$ exhibited a significant increase in NOE intensity with Ala64-CH_3 in the presence of CAP-1. These changes indicate that, upon CAP-1 binding, the His62 side-chain no longer packs against Val27 and Val59, but instead interacts with the N-terminal end of helix H4. In addition, Phe32 H^{ζ} undergoes a large upfield shift (from 6.81 ppm to 6.57 ppm) and exhibits increased NOE intensities to His62-$H^{\delta 2}$ and -$H^{\varepsilon 1}$ upon CAP-1 binding, indicating that the Phe32 side-chain packs against the side-chain of His62 in the CAP-1:CA^N complex.

CAP-1 precipitates at concentrations above 3 mM, and the maximum CA^N:CAP-1/CA^N(free) ratio achieved in the 2D NOESY experiments was therefore ~75%/25%. Under these conditions, Phe32 exhibited diminished but detectable NOEs with Trp23, Val36 and Leu138 due to rapid exchange between the CA^N (Phe32 sequestered) and CA^N:CAP-1 (Phe32 exposed) species. Well-resolved intermolecular NOE cross-peaks were also observed upon addition of CAP-1 to CA^N, including NOEs between CAP-1 H6 and the methyl protons of Val27, Val59, Ala65 and Met66; CAP-1 H3 and H5 NOEs to Val27 and Ala31; and CAP-1 C1-methyl NOEs to Trp23, Val59, Ala65, Leu138 and Ile141 (Figure 2). These data are consistent with a unique binding mode, in which the aromatic ring of CAP-1 is

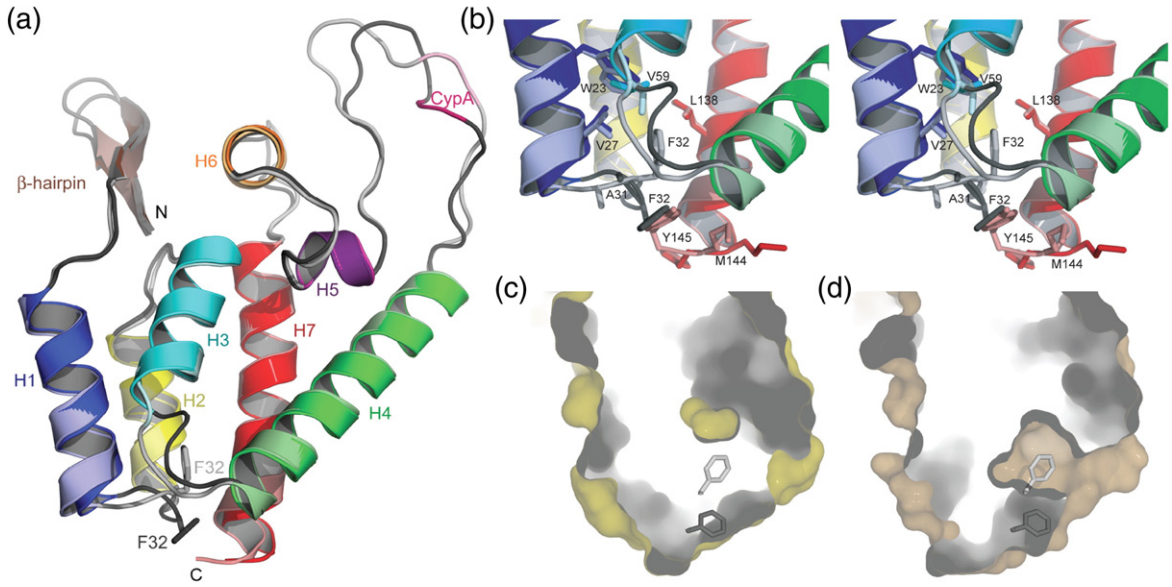

Figure 1. Structural changes induced in CA^N when crystallized in the presence of CAP-1. (a) Ribbon diagram of CA^N crystallized in presence (darker colors) or absence of CAP-1. Phe32 is shown explicitly. N and C termini, secondary structural elements, and the cyclophilin A binding site are labeled. (b) Close up stereo view of the structural changes in the presence of CAP-1. (c) Surface representation of CA crystallized in the absence (left) and presence (right) of CAP-1. Phe32 is shown explicitly in the open and closed conformations.